USING SCANNING ELECTRON MICROSCOPY TO MEASURE AIR PARTICULATES

By

LI YUN LO

A thesis submitted to the Department of Biology in partial fulfilment of the requirements for the degree of Bachelor of Science (Honours)

This thesis has been accepted by:

Chair, Department of Biology

Dean of Science (Interim)

Department of Biology
University of Prince Edward Island
Charlottetown, Prince Edward Island

May, 2019

Abstract

The importance of air particulates is often overlooked. Yet, it is crucial to the health of humans and other animals alike. In this study, a method of measuring air quality is proposed, using a scanning electron microscope (SEM). To determine whether this is an effective way of measuring particulate matter (PM) level in the air, roads with various substrate composition and ambient surroundings were selected to simulate various air conditions. Indoor air quality within specific buildings on the UPEI campus was also measured to further test this method. Air particles that settled on metal stubs at the various study sites were counted using a SEM. In terms of replicability, three, blind trials were performed for all the SEM photos taken. Correlation values for these trials were all above 0.7, indicating a strong, linear correlation coefficient r. In terms of this method's reliability, however, we learned that correlation values decrease as the number and the size of the particles decrease. Finally, for the indoor air samplings, the correlation coefficient between Dylos monitor and SEM count were weak and negatively correlated, indicating little to no correlation between the two data sets. In conclusion, as a stand-alone method, SEM is not as effective as previously anticipated. However, it does offer information towards the physical appearance of the particulates, which can provide valuable insights towards the air we breathe.

Acknowledgments

Special thanks to Professor Lacroix and Professor Teather for kindly providing funds and lab space for this project, in addition to the help they provided prior, during, and after the sample collection process. Thank you to Professor Peach-Brown for providing advice on this thesis and for being on the Supervisory Committee. Thank you also to Professor Hale, who provided feedback for the finalized version of this document.

Table of Contents

INTRODUCTION

The Earth's atmosphere is dynamic, consisting of various substances. Even in its 'purest' form, the atmosphere is a mixture of various gases, consisting of oxygen (21%), nitrogen (78%), argon (1%), as well as water and carbon dioxide (Seinfeld and Pandis, 2016). Besides these main gases, there are also trace gases and air particulates in the atmosphere. While this study mainly focusses on these particulates, it is important to note that the trace gases, as well as water vapour, have a complex relationship with air particulates. Air particulates act as sites of reaction for chemicals in the air, and also as carriers for pollutants (Kampa and Castanas, 2008). Particulates also have a complex relationship with weather and climate. They aid in the formation of clouds by acting as nuclei for water vapour in the air. However, particulates can also prevent the formation of rain, depending on the regional amount being suspended (Kampa and Castanas, 2008).

There are two main sources of atmospheric particulate matter (PM). One comes from natural events, such as volcanic eruptions, forest fires, and dust storms (Seinfeld and Pandis, 2016). Things like fungal spores and pollen are also an important natural source of air particulates. Particulate matter can also be produced from anthropogenic activities, such as gaseous waste emissions from factories, ash production from mining, biomass burning for agricultural or cooking purposes, and mobile vehicle emissions and ground disturbances (Seinfeld and Pandis, 2016). Particulates that originate from anthropogenic activities are generally more toxic and harmful compared to particulates

originating from natural events. These toxic compounds in the atmosphere can change the pattern of the Earth's climate (Seinfeld and Pandis, 2016) and ultimately circulate back to affect the health of the human population.

Since the Industrial Revolution, anthropogenic activities have resulted in significant increases in the amount and the type of trace particulates in the air (Seinfeld and Pandis, 2016). However, for a long period of time little attention was given to air particulates, as they were considered to be remote and nonreactive. It was not until various human health issues associated with atmospheric pollution began to appear that air particulates were noticed. The Great Smog of London in 1952, for instance, was one of the most important events in history that raised worldwide awareness about the impact of air pollution (Bell et al., 2004). The effect of the smog was linked to a sharp increase in morbidity and mortality rates in London at the time (Bell et al., 2004). Even during the months following the clearing of the smog, mortality and morbidity still remained at a higher rate compared to the time prior to the Great Smog. Today, it is recognized that air particulates play a crucial role in the complex relationship between environment and human health.

Air Particulates Overview

Air Particulates

Air particulates can be generated generally by two events: natural events and anthropogenic activities. However, this categorization can become increasingly plausible as it is now realized that human activities can have a ripple effect on natural phenomena.

For instance, human activities have led to global warming, and subsequently led to an increase in frequency and intensity of many natural events, such as hurricanes and droughts (Seinfeld and Pandis, 2016). Weather conditions such as these can disturb the soil and change the particular matter (PM) concentration in the air dramatically. Besides climatic events, anthropogenic activities, including mining, burning of biomass for agricultural or cooking purposes, fuel use, as well as construction and transportation, also affect the regional PM levels in the air (Seinfeld and Pandis, 2016). Although PM contributed by natural events can be harmful, especially in large concentrations, it is really the particulates originating from anthropogenic activities that have caused the most harm to both the environment and human health, due to the nature and size of these pollutants.

Depending on the size and the amount present, air particulates can exert a direct effect on human health. However, in other cases, air particulates act as carriers of toxic compounds into the human body. According to Jia et al. (2018), vehicle emissions are a major source of air particulates along roads and in big cities, such as Shanghai. Volatile organic compounds (VOCs), a group of organic compounds that are highly volatile at room temperature, can be emitted from the exhaust of vehicles, along with carbon monoxide and residual particulates from the combustion process (Jia et al., 2018). The VOCs act as irritants and affect the respiratory system of humans (Kampa and Castanas, 2008). VOCs with benzene attached can also be carcinogenic (Kampa and Castanas, 2008). Carbon monoxide (CO) is another toxic byproduct of fossil fuel burning (Jia et al., 2018). Due to a higher preference for CO binding in hemoglobin instead of oxygen (O_2),

relatively small amounts of CO can lead to death (Vallero, 2014). Prolonged carbon monoxide exposure can also lead to chronic cardiovascular issues (Vallero, 2014). These gaseous compounds can easily be inhaled by pedestrians along with air particulates. Furthermore, heavy metals have also been found in road side particulates in a previous study performed in Taiwan (Lin et al., 2005). Traffic-related air particulate studies have become an important topic in countries with heavily populated cities.

Air particulates from biological sources are also possible. These include microbial organisms like molds, fungal spores, and pollen grains (Kampa and Castanas, 2008). Many viruses and bacteria also use air particulates as a way to spread between hosts (Bell et al., 2004). Microscopic drops of infected fluid from a host can be suspended in the air and be inhaled by people nearby. Depending on the activities of pedestrians, wildlife, and domestic livestock, the dust in the air may also contain animal hair, particles deposited from feces and urine or bodily fluids, as well as dead skin cells. Although the presence of biological air particulates is often associated with poor indoor air quality, under certain circumstances, these microbes can also be a significant health concern outdoors. In the summer of 2011, a dust storm swept through the State of Arizona, United States. Along with the soil displaced, a type of soil fungus, *Coccidioides immitis*, was also carried into the air, affecting thousands of people within the region. According to Tong et al. (2017), the cases of Coccidioidomycosis, also known as Valley Fever, recorded between 2000 to 2011 increased over eight times its original value.

Valley Fever is caused by the inhalation of soil-dwelling fungal spores (Sprigg et al., 2014). Its size is about 5 µm, small enough to be lifted into the air with little wind

and remain suspended for a prolonged period of time (Sprigg et al., 2014). For about two thirds of the people infected, only slight symptoms developed. However, for the remaining one third of the people, the spores caused months of skin irritation and shortness of breath (Sprigg et al., 2014). In some cases, it can even be fatal. Within the population, the elderly and the younger generations, as well as pregnant women and immunocompromised people can be severely impacted by this infection (Brown et al., 2013). Valley Fever has been an ongoing health concern in certain states in the US during windier months.

Particle size range

There are three main PM categories: ultrafine, fine, and coarse particles (Taiwo et al., 2014). Ultrafine PMs consist of particles with a diameter of less than 0.1 µm. Fine particles are particles with a size between 0.1 to 2.5 µm. Coarse particles have a diameter between 2.5 to 10 µm. Any particulate larger than 10 µm can also be grouped under coarse particulates. It is also possible to have nano-sized PMs, ranging in size from 10 nm to 56 nm (Lin et al., 2005).

Coarse particulates are created mostly through abrasion or disintegration of larger particles (Taiwo et al., 2014). They are usually things like sand, pollen, or aggregation of various smaller particles. Fine and ultrafine particulates found along roads can have several origins (Taiwo et al., 2014). Inorganic substances like fine sand and silt are a source of fine particulates on a dirt road. Things like fungal spores, soot, chemical pollutants, tobacco smoke residues and mold are also considered fine particulates

(Taiwo et al., 2014). Fine particulates can also originate from vehicle emissions (Taiwo et al., 2014). If there are factories nearby, emissions are also a major source of fine particulates within the region (Taiwo et al., 2014). Although both the coarse and fine particulates are inhalable and can cause disease, the fine particulates are especially problematic, as they are able to penetrate lung tissues and be absorbed into the bloodstream (see Section 3).

Relationship between Climate and PM

One of the most important variables in the study of air particulates is climate. Depending on a region's weather, which encompasses the local atmospheric pressure, humidity, cloud cover, temperature, and many other factors, PM levels can fluctuate daily, even hourly at times. Drier air and regional disturbance can lead to more dust being suspended in the air. Wind circulation distributes particulates from one area to another, as in the case of Valley Fever (Sprigg et al., 2014). Solar radiation can also influence PM levels in the air. Photochemical reactions can produce more diverse particulates in the air, with particulates acting as a catalyst (Seinfeld and Pandis, 2016). An example would be the intricately linked relationships between oxides of nitrogen (NO_x), volatile organic compounds (VOCs) and ground level ozone (O_3) (Seinfeld and Pandis, 2016). Under normal circumstances, O_3 is produced via the splitting of oxygen by solar radiation, and this process can only occur in the stratosphere (Seinfeld and Pandis, 2016). It was discovered that tropospheric ozone can also be formed by photochemical reactions between atmospheric O_2, NO_x and VOCs at high temperatures in the presence

of sunlight and heat. Both NO_x and VOCs are the gaseous wastes of fuel combustion in vehicles (Seinfeld and Pandis, 2016). Although ozone in the stratosphere is beneficial to life on Earth, within the troposphere it is a direct hazard to vegetation and human health (Seinfeld and Pandis, 2016). Ozone is a very unstable chemical species that promotes oxidation with almost everything, ranging from metals to organic tissues (Kormondy, 1995). Numerous studies have been performed to study its effects on human health. Exposure to tropospheric ozone can lead to irreversible damage to lung structure. Symptoms can range from coughing to chest pain to death (Kormondy, 1995).

Air particulates are intricately linked to climate patterns. Particulates can cool or warm the atmosphere directly by absorbing or reflecting solar radiation. They can also influence the behaviour of clouds, depending on their sizes. In cloud physics, when an ultrafine or fine particulate becomes activated, or has gained the ability to attract water vapour, it becomes what is known as a cloud condensation nucleus (CCN) (Zhang et al., 2006). These nuclei are extremely small, typically with a diameter of less than 1 μm, and are crucial for the formation of precipitation. For every raindrop, icicle and snowflake formed, a cloud condensation nucleus is needed to act as the centre point for water vapour in the air to aggregate (Zhang et al., 2006). Water vapours condense on the surface of CCN, forming cloud droplets. These cloud droplets then aggregate together to form a raindrop, or a snowflake (Zhang et al., 2006). This might give the false impression that the higher the concentration of fine particulates in the air the better. However, this is not the case. With the same amount of water vapour in the air, an excess of fine particulates would reduce the likelihood of larger raindrop formation, as the water

vapour is being distributed amongst more CCN. This leads to high number of cloud droplets, but most of them would dissipate before reaching the ground since they are too small (Zhang et al., 2006). Thus, while fine particulates are beneficial to form precipitation, high amounts of fine particulates can have an opposite effect (Zhang et al., 2006). Precipitation can be reduced when the water vapour in the air is limited.

Health Impact of Particulate Matter

There are several ways in which air particulates can enter a human body: through skin absorption, ingestion, and inhalation. Skin absorption is not common, unless air particulates are extremely small and are able to penetrate several layers of dead skin cells (Kampa and Castanas, 2008). Compared to dermal absorption, ingestion is a more common route of entry for air particulates. Depending on the nature of the particulates involved, ingestion can lead to toxic exposure. For example, if the consumed food has been exposed to mold or other bacterial contaminated air, food poisoning can result (Kampa and Castanas, 2008). The most direct way that air particulates affect human health is through inhalation.

The filtering system of the human respiratory system is fairly efficient. Most coarse particles can be filtered out of the inhaled air via a healthy human respiratory system. They are deposited in the mucous secreted in the upper respiratory tract and are carried out of the respiratory tube via the ciliated cells that line the trachea (Lin et al., 2005). However, for smaller particulate matter, reaching the lower respiratory tract is easily achievable (Lin et al., 2005). These finer particulates are able to reach the alveoli in the

lungs and may often diffuse into the bloodstream (Kampa and Castanas, 2008). If particulates consist of toxic metals like mercury, zinc, strontium, and other transition metals, inhalation of the air particulates can be very toxic to humans. A study carried out in Ontario, Canada demonstrated how sediments (and ultimately PMs) were contaminated with various transition metals (Stone and Marsalek, 1996). In another study, the ultrafine particulates obtained along a busy street also contained transition metals that were associated with fuel and gasoline exhausts (Lin et al., 2005). These particulates can be easily absorbed by pedestrians walking along the roads.

Due to the highly variable effects of airborne particles, there is still much to be learned about their relationship with human health. However, based on previous studies, the size and the surface area to mass ratio of the particulate matter (PM) are strongly associated with the PM's ability to act as carriers and to cause disease (Kampa and Castanas, 2008). The smaller the particulates, the easier it is for them to reach deeper within the lungs. As mentioned before, coarse particulates can be filtered out efficiently and be deposited in the upper respiratory tract. This does not exclude the coarse particulates causing health-related issues, as some coarse particulates do have the potential of producing diseases. When coarse particulates are airborne, they tend to be deposited in the tracheobronchial region (Cui et al., 2018). At times, coarse particulates can carry traces of metals that can affect the upper respiratory tract (Cui et al., 2018). Although small in likelihood, as coarse particulates are more effectively filtered out compared to fine particulates, this can contribute towards weakening respiratory functions. Fine particulates are more likely to cause health issues. Compared to the

same amount of coarse particulates with the same mass, finer particles have a larger net surface area to mass ratio, which increases the amount of air pollutants that can be absorbed onto their surfaces. Consequently, a group of finer particulates are much more efficient at absorbing pollutants and are much less likely to be filtered out (Kampa and Castanas, 2008).

The degree of influence that air particulates have on human health depends on the concentration of air particulates inhaled, the length of exposure time, and the interactions between particulates and between particulates and humans (Kampa and Castanas, 2008). Symptoms of distressed airway include irritation of the nose and throat, constriction of the bronchi, and pneumonia (Kampa and Castanas, 2008). Emphysema and lung cancer can also result from exposure to polluted air particulates (Kampa and Castanas, 2008). Considering that air particulates can absorb various chemicals that are harmful to humans, the effects of $PM_{2.5}$ (particles that are smaller than 2.5 μm) have the potential to be detrimental to the respiratory system. People who are most affected are those with pre-existing respiratory and/or circulatory diseases. Elders, as well as children within the population are also affected by polluted atmosphere (Kampa and Castanas, 2008).

Several factors come into play in determining the severity of exposure to air particulates. The concentration of particulates in the air, the duration of exposure, as well as the types of particulates and pollutants being inhaled are all important factors to consider (Kampa and Castanas, 2008). In addition, the fact that humans are constantly breathing in a mixture of various substances can make pinpointing the exact source or

cause of a disease challenging. Nonetheless, based on previous studies, it is evident that an increase in air pollutants can lead to an increase in mortality and hospitalization (Kampa and Castanas, 2008).

Allergic reactions and asthma attacks can result from both prolonged and acute exposure to air particulates. Many things can induce an allergic reaction, ranging from exposure to pollen to exposure to bacterial and fungal spores, or their secreted toxins in the air (Griffin and Kellogg, 2004). One of the largest sources of atmospheric PM is produced by the Sahara Desert in Africa, and its dust particles are constantly being circulated around the globe and can act as an irritant that triggers asthma attacks. In recent years, its effects are even more pronounced as its boundary is gradually expanding due to deforestation and global warming, affecting millions of lives in the Mediterranean and Sudano-Sahelian regions of Africa (Darkoh, 1989). Not only are the dust particles affecting the local people within Africa, it is also affecting the people on the other side of the Atlantic Ocean, specifically the Caribbean region.

A study was performed in the Caribbean region to examine the relationship between Saharan desert dust and local pediatric asthma cases (Gyan et al., 2005). According to this study, the increasing trend of asthma between the years of 1970 and 2000 happened to coincide with increased amounts of Saharan desert dust in the Caribbean atmosphere. A 14% increase of pediatric asthma cases in Barbados was observed when the atmospheric Saharan dust levels became elevated. Wind circulation in the atmosphere causes large amounts of the dust from the Saharan desert to be deposited in the Caribbean region, carrying large amounts of pollen, vegetation

fragments, and microbes along with the desert clay. Similarly, in Southern Florida, about half of the fine particulates found in the summer months also originate from Africa (Griffin and Kellogg, 2004). Approximately 900 million kg of soil is circulated in the world's atmosphere annually. For every gram of soil in the air, about ten thousand bacteria can be carried along with it (Griffin and Kellogg, 2004). In addition, spore forming bacteria and fungi, and sometimes viral particulates are able to survive long distance air travel (Griffin and Kellogg, 2004). The PM's ability to provide an attachment surface area for various compounds and substances is important to consider when studying PM's effects on human health. Regardless of the air particulate concentration, air pollutants can impact the health of an individual.

Canada and Prince Edward Island

With the warming of the globe and the increased usage of motorized vehicles, careful air particulate monitoring is needed. To combat and to improve the air quality in Canada, the Canadian Ambient Air Quality Standards (CAAQS) were established in 2012 (Government of Prince Edward Island, 2014). The Air Zone Management Framework (AZMF) has been developed to monitor air particulate concentration (Fig. 1). There are four categories within AZMF; each category is colour coded with a range of annual $PM_{2.5}$, a range of 24-hour $PM_{2.5}$, as well as a range of parts per billion (ppb) for tropospheric ozone (Government of Prince Edward Island, 2014). The severity of the air quality increases from green level to red level.

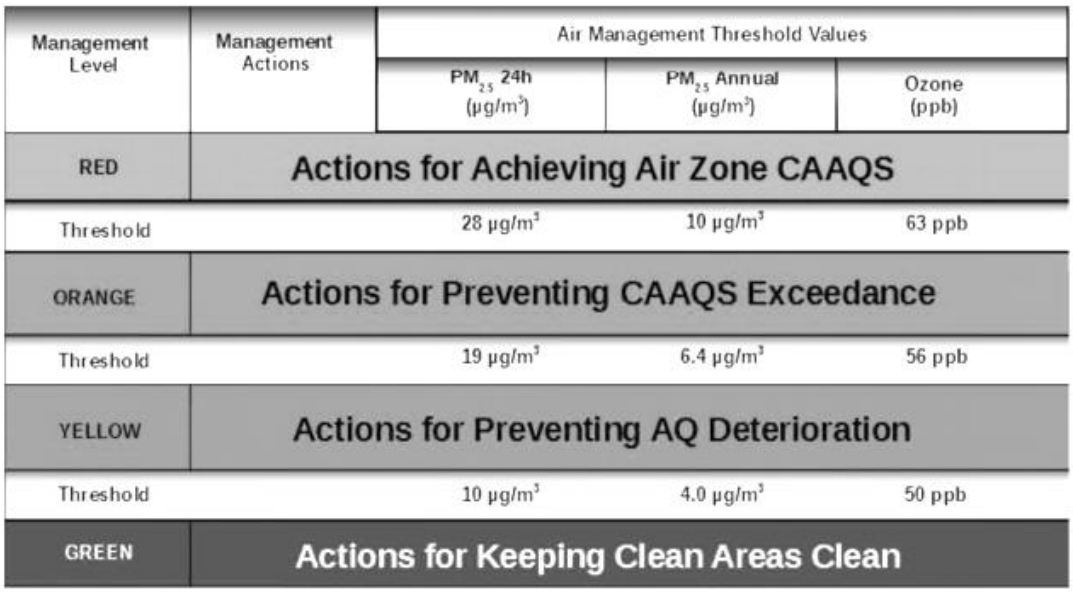

Management Level	Management Actions	Air Management Threshold Values		
		$PM_{2.5}$ 24h ($\mu g/m^3$)	$PM_{2.5}$ Annual ($\mu g/m^3$)	Ozone (ppb)
RED	Actions for Achieving Air Zone CAAQS			
Threshold		28 $\mu g/m^3$	10 $\mu g/m^3$	63 ppb
ORANGE	Actions for Preventing CAAQS Exceedance			
Threshold		19 $\mu g/m^3$	6.4 $\mu g/m^3$	56 ppb
YELLOW	Actions for Preventing AQ Deterioration			
Threshold		10 $\mu g/m^3$	4.0 $\mu g/m^3$	50 ppb
GREEN	Actions for Keeping Clean Areas Clean			

Figure 1. Air Zone Management Framework (AZMF) provided by the Prince Edward Island Air Zone Report 2014. (Government of Prince Edward Island, 2014)

According to the 2014 air zone report for the Island, the 24-hour $PM_{2.5}$ level and the average annual $PM_{2.5}$ has reached the yellow zone of air quality in the years between 2011 and 2013, with the values of 12 $\mu g/m^3$ and 5.2 $\mu g/m^3$, respectively (Government of Prince Edward Island, 2014). Both of these values put the island's air quality within the Yellow Zone, where air quality is not considered polluted yet, but it is undergoing deterioration. Since there are few factories on the island, vehicle traffic is an important source of PM here. The main source of pollution on the Island comes from local traffic as well as traffic resulting from tourism activities (Government of Prince Edward Island, 2014). No other source of pollutant was mentioned.

Study Focus

Breathing is crucial for us; yet, we know little about the composition of our air, particularly the particulate matter (PM) that can be inhaled readily into our bodies. These particulates were first thought of as inert substances. However, they have since been recognized as important players in both the fields of environmental pollution and human health.

A challenge in studying air particulates is their highly variable nature. Depending on the weather conditions within a region, such as the humidity, cloud cover, temperature, and wind speed, the amount of air particulates changes significantly. The Valley Fever case (Sprigg et al., 2014), for instance, demonstrated how interconnected climate is with air PM level. Furthermore, anthropogenic activities also contribute to the highly variable air particulate concentrations from region to region, specifically the

exhausts produced by vehicles (Seinfeld and Pandis, 2016). Even on a local scale, air particulate level can fluctuate drastically between two locations that are only a few meters apart.

There have been many studies performed on the dynamic roles of air particulates. Most of the studies rely on costly instruments and complex procedures. In a study of Jokhang temple air quality in China, for instance, a particle separator, which is costly and inaccessible for the general population, was used to collect particles based on their sizes (Cui et al., 2018). There are also portable and user-friendly air monitors available, such as Particle Counter Dust Measuring Device (PCE-PCO), and the Dylos monitors. However, none of these monitors allow users to look at the particles up close.

In this study, the SEM was used to quantify and qualify particulate samples collected from various places that are known to be associated with high levels of dust, or that are typically frequented by people. To determine whether a SEM stub count is an effective way to quantify local PM levels, the counts were compared with two Dylos 1700 laser particulate samplers. The samplers detect two size categories: particles above 0.5 μm in size and particulates that are above 2.5 μm. To compare these two methods, unpaved roads were chosen to carry out the experiment. The second objective was to use the SEM in an attempt to assess the PM level in places frequented by people on the University of Prince Edward Island campus. By comparing these data, the effectiveness of using SEM to quantify and qualify air particulates could be tested. We hypothesized that roads that are less compact, such as dirt roads, would have a higher amount of PM compared to paved roads. We also expect that denser vegetation covers would generate

a greater diversity of particulates. Finally, we hypothesized that indoor PM levels would be highest in areas of high traffic, such as the library hall.

METHODS

In this study, the SEM is proposed as a complementary method to quantify air particulates.

Collection Box Preparation and Stand Setup

Collection boxes for the SEM stubs were prepared for sampling (Figure 2a). They were wiped with 70% ethanol and air-sprayed using Fisherbrand's Super Friendly Air'it. To minimize dust within the containers, boxes were placed in an upside-down position on Kimwipes after being cleaned. The SEM stubs used were all new and taken from unopened bags using gloves and a tweezer. These stubs were air-sprayed after they were taken out and an adhesive film was quickly placed on each stub. Two stubs were placed within each box at opposite ends from each other, and the box was air-sprayed again before being sealed with Parafilm. A collection was also prepared with two levels to place the collection boxes and the Dylos monitors (Figure 2b).

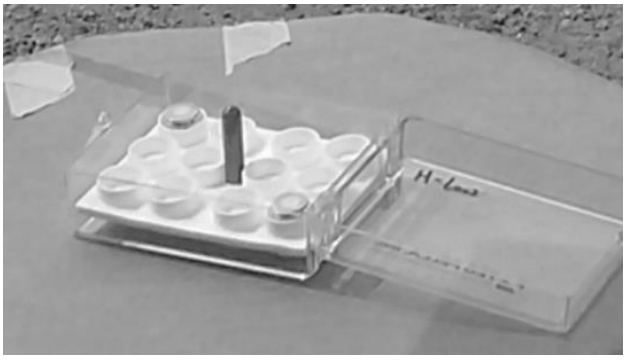

Figure 2a. SEM collection box with two tubs within during sampling.

Figure 2b. Collection stand with two collection boxes and Dylo monitors placed on it.

Road Sampling

Eight roads were sampled, varying in the degree of vegetation coverage and the road composition (Figure 3). They ranged from gravel roads, which were dusty, to completely paved roads that had little dust (Table 1). In addition, vegetation covering, the amount of vegetation covering above the road surface, was also described for all sites in the Table. In order to minimize the effect of weather, samples were collected after two days of warm weather and during the warmest part of the day, and little wind was evident. Sampling took place on two occasions; once in July and at another time in August. For each site, a five-minute sampling period was used along the edge of the road. The first minute was timed after containers were opened and monitors turned on. At the one-minute mark, a vehicle passed by the stand five times, with 30 second intervals between each pass to increase the amount of air particulates. After the last pass, two minutes were allocated to allow dust to settle before the monitors were turned off and the boxes were closed.

Figure 3. Photos of the sampled sites.

Table 1. Description of the road conditions and surroundings for each sample site. Vegetation covering is the degree of vegetation growth around sample sites.

Sites	Road condition	Degree of vegetation coverage
A	Unpaved, gravel	On the side only
B	Unpaved, dirt	Overhead covering
C	Unpaved, dirt	Overhead covering
D	Paved	Short, lawn grass
E	Unpaved, dirt	On the side only
F	Unpaved, gravel	On the side only
G	Unpaved, sand	On the side only
H	Semi-paved	Short, lawn grass

SEM Preparation and Viewing

To view the stubs under the SEM (Figure 4a), a fine, metallic coating was added onto the stubs before viewing. The coating was added using a Desk II Sputter Coater (Figure 4b). Prior to setting the stubs into the machine, the machine was cleaned with air-spray. All four stubs from the same site were coated together. The duration of the coating process was seventy-five seconds at a current of 40milliAmps. This resulted in a coating thickness of 300 angstroms. Once they were coated, the stubs were placed back into their original containers, and Parafilm was used again to seal the container until samples were ready to be viewed.

Figure 4a. Hitachi TM3000 Tabletop Scanning Electron Microscope used for this project.

Figure 4b. The Desk II Sputter Coater used during coating.

Determining Particle Nature

SEM photos were taken for all stubs viewed, including close-up particle photos using varying levels of brightness and contrast. For particle counts, two SEM photos were taken at 100x magnification for each stub: centre view and left of centre view. Since the SEM stubs were round, these two viewing planes were chosen so that the viewing procedure is consistent for all stubs. With the sheer number of particles that needed to be counted, 100x magnification was considered to be a reasonable trade-off that would not magnify large particles too much, while still including many of the smaller particles. Each visible particle was counted starting from top left corner of the viewing grid to the bottom right corner. Particles that were questionable or blurry were not counted. Particles smaller than 5 µm were also not counted, as they would be too small to be seen easily. Only particles that were clearly visible under 100x magnification, or small particles visible as a bright point were counted.

Statistical Analysis

To test the consistency of the EM count, two Dylos 1700 laser monitors were used. However, one of them malfunctioned during the sampling process. Thus, only data from one monitor was used. Two sets of data were produced by the monitors, particulates that are larger than 0.5 µm ($P_{>0.5}$) and particulates that are larger than 2.5 µm ($P_{>2.5}$).

Microsoft Excel 2010 was used to record and interpret data, as well as produce tables and graphs. The Pearson's correlation coefficient in Excel was used for correlation

analysis. Positive value indicates that data sets were aligned; negative value indicates data trends were inversely related. Values closer to zero indicates weak correlation. The closer the value I to 1, the stronger the linear relationship is (Zhou et al., 2016). In this study, a positive value indicates a linear relationship, and would indicate similarity between data sets.

To determine the method's replicability (i.e. how consistent the counts using the SEM were), three counts were performed for all photos, and correlation coefficient test was performed. To determine the method's reliability (i.e., its ability to estimate the number of air particulates), the averages of the high stub counts were compared to the five-minute averages of the Dylos data. A strong, positive correlation would indicate that the SEM counts could be used to reliably predict the number of air particles.

Indoor Air Sampling

Four, on-campus buildings were selected to conduct the samplings. The buildings were Duffy Science Building (F), Kelly Building (G), Robertson Library Building (H), and Main Building (I) (Figure 5). These buildings were chosen because these are a few of the places where students and staffs visit frequently. Thus, I was curious to see what the air quality is like within these buildings. Each site was tested twice: once during quiet hours, and another during busy hours when students were moving around between classes. All samples, for both busy and quiet hours, were collected on the same day. The collecting method was similar to road sampling, except people were allowed to walk in front of the stand during the five-minute period.

Figure 5. On campus sample sites. From left to right, the sites were Duffy Science Building lobby, second floor in Kelly Building, Library hallway, and third floor stairway in St. Dunstan's Main Building.

RESULTS

The main purpose of sampling various road conditions is to simulate various air particulate amounts. In addition, I wanted to determine if there was any difference in the nature of the particles when sampling sites varied in terms of surroundings. The expected order of air particulate generation, ranging from highest to least number of particulate matter, is as followed: unpaved, dirt roads (sites B, C and E) to unpaved, sand road (site G) to gravel roads (sites A and F) to semi-paved road (site H) to paved road (sites D).

In both sample times, only the paved road (site D) had a low SEM count average compared to the rest. The semi-paved road (site H) also remained low for both samplings. Other sites had varied between the two sample periods, with sites B, C, F and G being the ones with the highest difference. As different values were recorded at different sampling times, the correlation value was -0.2701 for July and August samplings, which indicated a weak correlation.

Replicability

The averages of the three trial counts for the first and second road samplings were presented in the Tables 2 and 3. Although the counts were performed by the same person, they were performed blindly on separate days. Pearson's correlation coefficient test was performed both road samplings. The ranges were 0.8242 to 0.9394 for the first road sampling, and 0.7720 to 0.9020 for the second road sampling.

Table 2. Average of three particle trial counts for the first road sampling (July 13, 2018). The high represents the stubs on the high level, and the low represents the stubs on the low level.

		Averages		
Summary		Centre	Left of Centre	Average
A.	High	52.0 (±20.8)	63.2 (±23.4)	57.6 (±21.9)
	Low	102.5 (±17.6)	109.2 (±29.2)	105.8 (±23.2)
B.	High	120.8 (±29.3)	125.5 (±41.0)	123.2 (±34.1)
	Low	166.3 (±16.5)	176.5 (±7.7)	171.4 (±13.4)
C.	High	126.8 (±26.5)	106.7 (±35.0)	116.8 (±31.4)
	Low	118.8 (±16.2)	131.5 (±22.7)	125.2 (±19.9)
D.	High	51.2 (±17.9)	65.7 (±20.0)	58.4 (±19.6)
	Low	65.0 (±41.6)	59.7 (±17.8)	62.3 (±30.6)
E.	High	53.8 (±19.3)	41.8 (±15.2)	47.8 (±17.7)
	Low	61.3 (±33.9)	65.8 (±15.3)	63.6 (±25.2)
F.	High	128.5 (±19.9)	123.2 (±11.7)	125.8 (±15.8)
	Low	160.3 (±23.1)	155.7 (±26.7)	158.0 (±23.9)
G.	High	39.8 (±15.7)	40.7 (±12.2)	40.3 (±13.4)
	Low	61.8 (±20.3)	57.0 (±18.3)	59.4 (±18.6)
H.	High	57.7 (±23.4)	58.7 (±25.9)	58.2 (±23.5)
	Low	58.3 (±24.7)	64.7 (±38.3)	61.5 (± 30.9)

Table 3. Average of the three particle trial counts for the second road sampling (August 1, 2018). The high represents the stubs on the high level, and the low represents the stubs on the low level.

		Average		
Summary		Centre	Left of Centre	Average
A.	High	38.5 (±9.6)	38.0 (±4.3)	38.25 (±7.1)
	Low	82.5 (±52.3)	70.8 (±47.9)	76.7 (±48.2)
B.	High	26.8 (±9.3)	21.0 (±9.9)	23.9 (±9.7)
	Low	29.7 (±9.3)	25.3 (±8.5)	27.5 (±8.8)
C.	High	21.0 (±5.7)	25.2 (±4.7)	23.1 (±5.4)
	Low	34.5 (±11.4)	32.7 (±2.0)	33.6 (±7.9)
D.	High	16.2 (±4.3)	16.8 (±6.0)	16.5 (±5.0)
	Low	16.2 (±4.6)	18.0 (±6.3)	17.1 (±5.4)
E.	High	36.0 (±8.1)	32.8 (±12.3)	34.4 (±10.1)
	Low	34.0 (±4.7)	36.7 (±10.2)	35.3 (±7.7)
F.	High	29.2 (±7.5)	24.3 (±6.9)	26.8 (±7.3)
	Low	38.5 (±1.0)	41.5 (±6.3)	40.0 (±4.6)
G.	High	74.3 (±4.3)	87.7 (±38.4)	81.0 (±27.0)
	Low	107.0 (±42.1)	110.5 (±41.9)	108.8 (±40.1)
H.	High	43.8 (±2.43)	33.2 (±19.4)	38.5 (±21.7)
	Low	44.8 (±16.1)	29.8 (±10.0)	37.3 (±15.0)

Relationship between the high- and low-level stubs

A two-levelled stand was used for sample collection to see if the PM collected would differ between the two levels. Both high and low level stubs had similar trends compared to each other. Between the high and the low stub averages, the correlation values were 0.9273 for the first sampling, and 0.9164 for the second sampling. In both cases, the low stubs consistently led to higher number of SEM particle counts compared to the high stubs (Figures 6a and 6b).

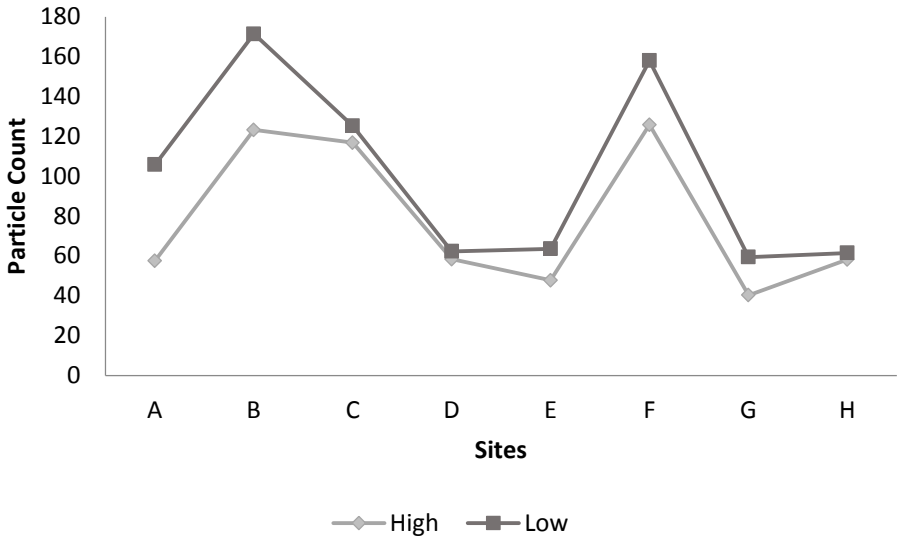

Figure 6a. Comparison of the high and low level stubs for the first road sampling. Correlation value between the high and the low stubs was 0.9273.

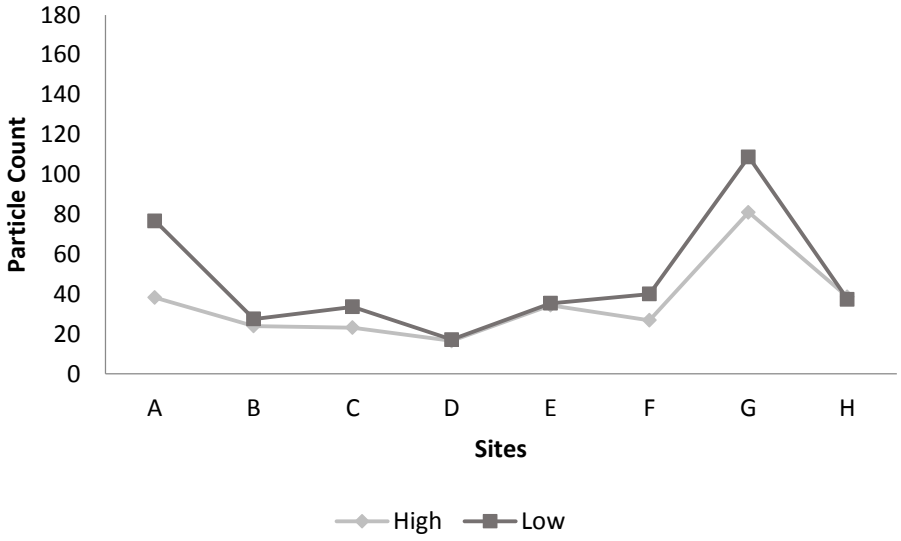

Figure 6b. Comparison of high and low level stubs for the second road sampling. Correlation value between the high and the low level stubs was 0.9164.

Reliability

To determine this method's reliability, in other words, how well this method could estimate for PM level in air, the SEM counts were compared to Dylos data. Figures 7a and 7b showed a comparison between the SEM count and Dylos data. As mentioned before, two data were generated by the Dylos: $P_{>0.5}$ and $P_{>2.5}$. For the first road sampling, the correlation values between the manual count and monitor A $P_{>0.5}$, and between manual count and monitor A $P_{>2.5}$ were 0.9089 and 0.9339, respectively (Appendix B). The correlation values for the second road sampling were slightly lower, with values of 0.6875 (with Dylos A $P_{>0.5}$) and 0.7693 (Dylos A $P_{>2.5}$). See Appendix C for detailed calculation.

The PM levels determined by the Dylos monitors can be estimated from the SEM samples having moderate to high amounts of large particles ($P_{>5}$). To estimate the $P_{>2.5}$ value in the air, the particulate count can be multiplied by 14.1. To estimate for the $P_{>0.5}$ value in the air, the particulate count can be multiplied by 23.2. These values were obtained using the first road sampling, since the data had higher correlation values compared to the second road sampling. The Dylos data was divided by the SEM count, and then averaged.

The purpose of dividing Dylos data by the SEM count was to find what the ratio was between the two values for each site. For instance, counting 57.6 particles in site A is equal to an average of 2862.6 $P_{>0.5}$ measured. Their ratio is 49.7, which means for every particle counted on the SEM, it would roughly equal to 49.7 $P_{>0.5}$ detected by the Dylos sampler. The same procedure was used to calculate $P_{>2.5}$ from SEM counts. There

is one assumption with this calculation, however: it was assumed that the ratio between the SEM and particle counts by the Dylos sampler would be fixed across sites. Although the ratio between the SEM count and Dylos data was not the same across all sites, the assumption can still be considered valid. This variation may be due to element influence, or the subtle difference in vehicle speed in each run that ultimately led to different PM detected, or particles were more concentrated in air away from the monitors. However, in order to minimize variable influence, another average was calculated using these averages (See Appendix A for calculations.)

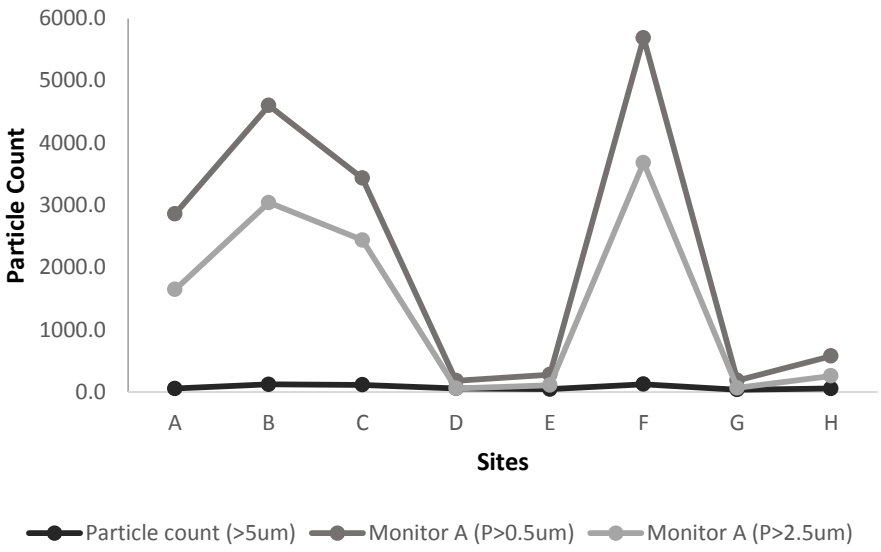

Figure 7a. Comparison between particle count and Dylos monitor A data ($P_{>0.5}$ and $P_{>2.5}$) for all sites on July 13, 2018.

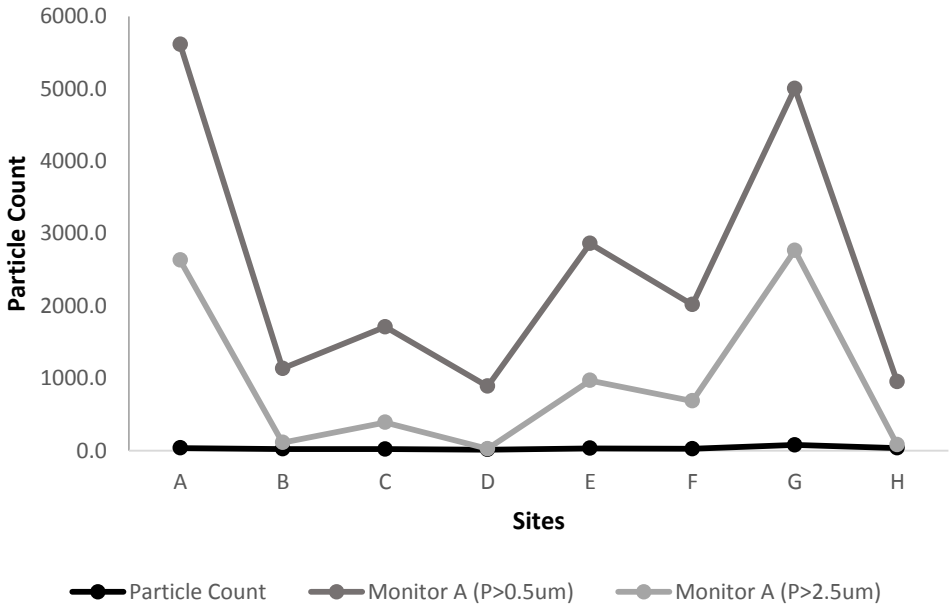

Figure 7b. Comparison between particle count and Dylos monitor A data ($P_{>0.5}$ and $P_{>2.5}$) for all sites on August 1, 2018.

Indoor Sampling

To validate the method proposed, the PM level within buildings on UPEI campus was sampled. Averages were recorded for the sample sites in (See Table 4). For the building sampling, the correlational values between the three counts ranged from 0.6585 to 0.8249 (Appendix D). Particle count values were relatively similar across four sites with no apparent relationship between the high and the low stubs. The Dylos data and SEM particle counts did not follow similar trends (Figure 8).

Table 4. Data of stub trial counts for indoor sampling (November 15, 2018). All sites included (A to H) for both busy and quiet environments. High stubs were labelled as High 1 and High 2, and similarly for stubs on lower level (Low 1 and Low 2). An average was taken for both the centre and left of centre viewing planes.

Summary		**Average**		
Busy		Centre	Left of Centre	Average
F.	High	38.7 (±11.4)	46.2 (±13.6)	42.4 (±12.6)
	Low	55.8 (±30.2)	53.2 (±16.0)	54.5 (±23.1)
G.	High	45.5 (±21.3)	58.0 (±13.9)	51.8 (±18.3)
	Low	55.0 (±20.3)	52.5 (±15.6)	53.8 (±17.3)
H.	High	53.0 (±22.0)	60.8 (±29.7)	56.9 (±25.3)
	Low	71.3 (±24.9)	75.0 (±24.8)	73.2 (±23.8)
I.	High	90.0 (±49.9)	90.0 (±62.7)	90.0 (±54.0)
	Low	68.8 (±26.9)	71.0 (±23.9)	69.9 (±24.3)
Quiet				
F.	High	61.2 (±22.1)	57.3 (±18.7)	59.3 (±19.6)
	Low	38.8 (±21.8)	44.0 (±36.5)	41.4 (±28.8)
G.	High	48.0 (±22.4)	57.5 (±19.6)	52.8 (±20.7)
	Low	38.2 (±19.6)	52.2 (±19.6)	45.2 (±20.1)
H.	High	76.8 (±42.6)	80.0 (±34.7)	78.4 (±37.1)
	Low	61.7 (±37.8)	60.8 (±24.3)	61.3 (±30.3)
I.	High	94.7 (±17.2)	77.8 (±13.7)	86.3 (±17.2)
	Low	62.3 (±16.7)	66.0 (±25.3)	64.2 (±20.6)

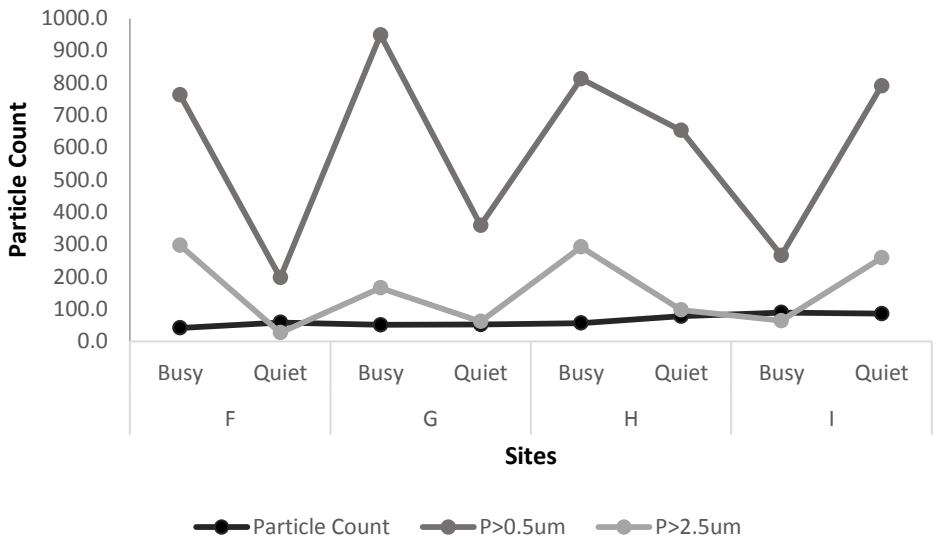

Figure 8. Comparison between particle count and Dylos monitor A data ($P_{>0.5}$ and $P_{>2.5}$) for campus sampling on November 15, 2018.

Types of Particle

Particles viewed were divided loosely into organic and inorganic categories. Organic particles were defined as particles that had likely originated from a living organism. These particles have a certain degree of symmetry, or a repetition of smaller subunits or protrusions (see Figure 9a). Anything else was categorized under inorganic, such as particles with irregular shapes, or crystalline appearances (see Figure 9b). Outdoor particles observed were mostly mineral based. In most cases, large particles had smaller particles attached to them. Some organic particles were also found; most were unidentified hair-like or bark-like materials. See Appendices G and H for photos. Similar to the outdoor samples, indoor samples were mostly inorganic as well. However, particles were more of a crystalline nature instead of mineral. Substances of a more fibrous nature were also found. See Appendix G for photos of indoor samples.

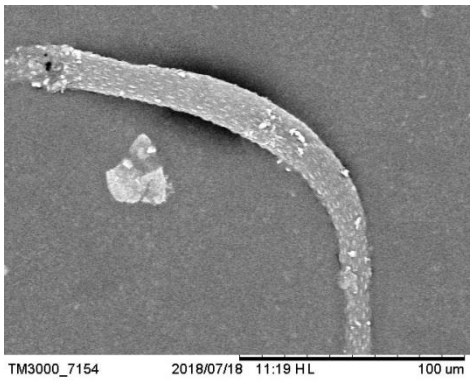

Figure 9a. Hair-like particle with fine extensions along its length classified as an organic particle.

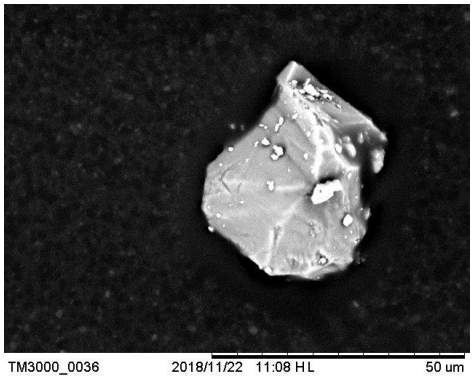

Figure 9b. Mineral-like particles with smaller particles attached onto it, classified as an inorganic particle.

DISCUSSION

In this study, an alternative or complementary way of determining the amount of air particulates, using SEM, was proposed.

Replicability

In order to determine whether this method is effective, we needed to determine whether using images generated by the SEM to count particles is able to be consistent. For both samplings, the correlation coefficient range was strong (0.8242 to 0.9394 for the first road sampling and 0.7720 to 0.9020 for the second road sampling). The strong correlation indicated a strong, linear trend between all trial counts. As mentioned for Pearson's correlation coefficient test evaluates the linear relationship between data sets. The stronger the relationship, the closer it is to 1, with +1 being data having identical, positive, linear relationship. Thus, values produced from the trial counts were indications of strong, positive, linear relationship between each other.

In both cases, the standard deviation values were also recorded. However, due to the size of the trial counts conducted, the wide range was not surprising, as standard deviation tends to decrease as the sample population increase (Naghshpour, 2012).

Reliability

To determine how well this method is able to estimate for PM level (i.e., how reliable this method is), the SEM count averages were compared to the Dylos data, and Pearson's correlation coefficient test was performed. If this method is reliable, then the correlation test would produce a high value that is closer to 1. If not, then the values would be closer to 0 (Naghshpour, 2012).

Visual particle counts were averaged and then compared with the data collected from Dylos laser air monitors. Due to malfunction of one of the monitors during sampling, only one monitor was used for this analysis. One main thing found for both samplings was that the SEM count and the Dylos data had similar trends (See Figures 7 and8). Therefore, it is possible to estimate the amount of PM in the air, by comparing the SEM count and the Dylos data. The two types of data generated by Dylos are important because by subtracting these values, particles that are within 0.5 µm and 2.5 µm can be estimated within the ambient air. Particles within this range have raised more health issues compared to coarse particles. As mentioned earlier, fine particles (P<2.5 µm) are more likely to reach deeper into lungs and diffuse into the bloodstream (Kampa and Castanas, 2008). Therefore, knowing the amount of fine particles in the air is crucial for human health, especially for people who have pre-existing respiratory or circulatory conditions (Kampa and Castanas, 2008).

Relationship between High and Low Stubs

As shown in Figures 6a and 6b, the high and low stubs showed high similarity in their trends, with the lower level stubs consistently led to higher SEM count compared to the higher level stubs. Their correlation values also demonstrated a strong, linear relationship (0.9273 for the first sampling and 0.9164 for the second sampling). Thus, we know from these graphs that it is possible to estimate the amount of PM level at the higher level from the values generated at a lower level. Thus, another way of reducing standard deviation, for future studies, could be by collecting samples closer to the ground.

Further Discussion

An important thing noted during analysis was that subjectivity increased as the amounts of large particles being viewed decreased. If there were no large particles being viewed, background texture was more likely to be mistaken for particles and counted.

The samplings were performed once in July and at another time in August. Since the number of particles varied across months for a particular place, and even within different times during a day, it is likely that there is tremendous variation across time even at specific sites. A study performed in the Caribbean region (Gyan et al., 2005), for instance, demonstrated how natural phenomena can influence PM level, and even the types of the particles, in the air. Similarly for this project, on a smaller scale, a shaded area (e.g. site C) can dry up more slowly compared to a fully exposed area (e.g. site D). Dirt roads can have a much more, varied PM generation because of this.

Indoor Sampling

The smaller the air particulate, the easier it is able to become airborne upon disturbance. Thus, the initial assumption was that busier environments would lead to a higher concentration of air particles. Looking only at the Dylos monitor, its data did support the hypothesis that busier environment lead to higher PM level as indicated in Figure 8. Other than in the Main building (site I), where the number of people was unusually higher than normal during the quiet hours compared to busier times, the Dylos monitor detected higher particle concentrations.

However, the SEM method did not support the hypothesis, as the counts remained relatively constant between the busy and the quiet times, as well as across the sample sites. Comparison between the particle count and $P_{>0.5}$, and between particle count and $P_{>2.5}$ were weakly correlated, with values of 0.1882, and 0.1095, respectively. One possible reason behind this would be the decrease in the amounts of large particles sampled and viewed. Particle counts using the TM3000 SEM were only able to view particles as little as 5 µm, under 100x magnification. Thus, a decrease in visible particles could lead to an increase in subjectivity, resulting in lower correlation values.

Particle Nature

The SEM was a good way to determine the nature of particles. However, it was harder to determine the nature of particles that were smaller than 5 µm, even under high magnification (i.e. magnification over 1000x). On the other hand, large particles ($P_{>5}$)

had clearly defined shapes. Thus, it was easier to distinguish the type of material the particles are made up of for larger particles.

Most particles viewed were inorganic in nature, or aggregates of smaller, inorganic particles. Outdoor particulates generally had a more mineral-based origin. Organic material, such as hair-like extensions and samples with a woody or tube-like appearance were also commonly found outdoor. Although pollen and spores were not observed, this may be due to the timing and the location where the sampling was conducted. Furthermore, the particles did not seem to vary in appearance across different vegetation covers. However, because this project only considered a small air volume for each site, further study may find supporting evidence for this hypothesis. As mentioned earlier, spores and pollen are commonly found in the air at particular times when plants are nearby (Griffin and Kellogg, 2004). In general, it was found that dirt roads would generate higher amount of visible particles compared to paved roads. See Appendices G and H for detailed explanation of outdoor photos taken. Similar to outdoor particulates, indoor particulates were generally inorganic as well. In addition to particles that are formed from aggregates of inorganic substances, crystalline as well as fibrous particles were also common. See Appendix G for photos of indoor particles examined.

CONCLUSION

The SEM particle count method has the potential of producing more consistent result, either through performing more trial counts, or examining more fields of view at higher magnifications. In terms of reliability, this method is not suitable as a stand-alone method. However, it can provide an acceptable estimation of particulates when a high number of large particles are present. As previously stated, an increase in subjectivity in identifying particles tends to happen when there are fewer large particles.

One drawback of this method is that counting particles under SEM is time consuming. Compared to the Dylos machine, which gives and records instant data, the SEM method requires manual counts that can take up to weeks to finish, depending on the sampled amount. However, it is important to note that visual particle counts can provide data that Dylos monitors cannot: the specific size and appearance of the particles being collected. These are valuable data that can provide evidence towards the origin of the particles in which we breathe. During viewing, many particulates were also found as aggregates of various materials. According to Griffin and Kellogg (2004), soil particles that are circulated within the atmosphere can carry substances like fungal spores, which can ultimately be inhaled by humans and animals alike. Thus, observing aggregated particles in this project further supported Griffin and Kellogg's statement.

If similar experiments were to take place in the future, it would be important to set a standard background and contrast for the SEM that would allow the viewing of

smaller particles, as the background used under 100x was only able to see particles as small as 5 μm. Furthermore, instead of examining the two photos for each stub three times, it might be better to perform only one count, but take at least five or more photos at a higher magnification across a stub. This could increase the accuracy of the sampling and give an estimation that is closer to the actual PM level.

An additional analysis that would be interesting to explore would involve determining the chemical nature of air particulates. In many studies performed previously on air pollutants, many included the analysis of compounds such as VOCs, tropospheric ozone level, and other toxic heavy metals. Heavy metals, in particular, have been found in the air samples collected along busy streets in Ontario, Canada (Lin et al., 2005). With the increasing Island population, along with the increasing traffic flow, I am curious to see if any of these substances are significant along main roads, such as University Avenue or roads within downtown area of Charlottetown, where people frequently visit. With the summer months approaching, people would also spend more time outdoors, but the air quality is still largely unknown. Thus, it is an important issue worth further examination.

In the few, existing studies that have used this type of microscope, many used it in combination of other tools for finer examination. An example of a complementary analysis with TM3000 would be the usage of an X-ray spectrometer (Orliukas, 2013), in which particles are examined for their chemical composition. Thus, by combining TM300 with other analyzing tools for future studies, it may be possible to identify the exact composition of the particulates and the substance(s) they carried.

References

Bell ML, Davis DL, and Fletcher T. 2004. A retrospective assessment of mortality from the London smog episode of 1952: The role of influenza and pollution. Environ Health Perspect. (1):6.

Brown J, Benedict K, Park BJ, and Thompson RG. 2013. Coccidioidomycosis: Epidemiology. Clinical Epidemiology. 2013(1):185-197.

Cui L, Duo B, Zhang F, Li C, Fu H, Chen J. 2018. Physiochemical characteristics of aerosol particles collected from the Jokhang temple indoors and the implication to human exposure. Environmental Pollution. 236:992.

Darkoh MBK. 1989. Desertification in Africa. Journal of Eastern African Research & Development. 19:1-50.

Griffin DW, and Kellogg CA. 2004. Dust storms and their impact on ocean and human health: Dust in Earth's atmosphere. Ecohealth. 1(3):284-95.

Government of Prince Edward Island. 2014. Prince Edward Island 2014 air quality report for the years 2011 - 2013.

Gyan K, Henry W, Lacaille S, Laloo A, Lamsee-Ebanks C, McKay S, Antoine RM, and Monteil MA. 2005. African dust clouds are associated with increased pediatric asthma accident and emergency admissions on the Caribbean island of Trinidad. Int J Biometeorol. (6):371.

Jia S, Yan G, Shen A. 2018. Traffic and emissions impact of the combination scenarios of air pollution charging fee and subsidy. Journal of Cleaner Production. 197:678-89.

Kampa M and Castanas E. 2008. Human health effects of air pollution. Environmental Pollution. 151(2):362-7.

Kormondy EJ. 1995. Tropospheric ozone: Human health and agricultural impacts. Boca Raton: Lewis Publishers.

Lin C, Chen S, Huang K, Hwang W, Chang CG, and Lin W. 2005. Characteristics of metals in Nano/Ultrafine/Fine/Coarse particles collected beside a heavily trafficked road.

Environmental Science and Technology. American Chemical Society: Washington DC. (21):8113.

Naghshpour S. 2012. Statistics for economics. [electronic resource]. 1st ed. ed. Business Expert Press.

Orliukas AF, Venckute V, Miškinis J, Kazlauskiene V, Petrulionis D, Šalkus T, Dindune A, Kanepe Z, Ronis J, Žukauskas T, et al. 2013. x-ray photoelectron and broadband impedance spectroscopy of li1+4xti2-x(po4)3 solid electrolyte ceramics. Lithuanian Journal of Physics. 53(4):244.

Rosenfeld D, Rudich Y, and Lahav R. 2001. Desert dust suppressing precipitation: A possible desertification feedback loop. Proc Natl Acad Sci U S A. (11):5975.

Seinfeld JH and Pandis SN. 2016. Atmospheric chemistry and physics: From air pollution to climate change (Third edition). Hoboken, New Jersey: John Wiley & Sons, Incorporated.

Sprigg WA, Nickovic S, Galgiani JN, Pejanovic G, Petkovic S, Vujadinovic M, Vukovic A, Dacic M, DiBiase S, Prasad A, and El-Askary H. 2014. Regional dust storm modeling for health services: The case of valley fever. Aeolian Research. 14:53-73.

Stone M and Marsalek J. 1996. Trace metal composition and speciation in street sediment: Sault Ste. Marie, Canada. Water Air and Soil Pollution. (1):149.

Taiwo AM, Beddows DCS, Shi Z, and Harrison RM. 2014. Mass and number size distributions of particulate matter components: Comparison of an industrial site and an urban background site. Science of the Total Environment. 475:29-38.

Tong DQ, Wang JXL, Gill TE, Lei H, and Wang B. 2017. Intensified dust storm activity and valley fever infection in the southwestern united states. Geophysical Research Letters. 44(9):4304-12.

Vallero D. 2014. Chapter 10 - cardiovascular effects of air pollutants. Academic Press: Boston. NA:257-69.

Zhang L, Michelangeli DV, and Taylor PA. 2006. Influence of aerosol concentration on precipitation formation in low-level, warm stratiform clouds. Journal of Aerosol Science. 37(2):203-17.

Zhou H, Deng Z, Xia Y, Fu M. 2016. A new sampling method in particle filter based on pearson correlation coefficient. Neurocomputing. 216:208-15.

Appendices

Appendix A. Calculations for deriving $P_{>0.5}$ and $P_{>2.5}$ from SEM particle count. Each of the Dylos data were divided by SEM count, and then averaged.

Averages	**SEM Particle count (P>5 µm)**	**Monitor A ($P_{>0.5}$ µm)**	**Monitor A ($P_{>2.5}$ µm)**	**Deriving $P_{>0.5}$ from SEM count**	**Deriving $P_{>2.5}$ from SEM count**
A	57.6	2862.6	1647.2	49.7	28.6
B	123.2	4601.2	3042.2	37.4	24.7
C	116.8	3436.6	2440.8	29.4	20.9
D	58.4	183.6	59.4	3.1	1.0
E	47.8	280.6	110.4	5.9	2.3
F	125.8	5688.4	3685.4	45.2	29.3
G	40.3	187.0	67.6	4.6	1.7
H	58.2	577.6	259.0	9.9	4.5
			Averages	23.2	14.1

Appendix B-1. Averages for the SEM particle count and Dylos monitor (first sampling data).

Site	High Stubs Average Count (1a)	Low Stubs Average Count (1b)	Dylos Count $P_{>0.5}$ (2)	Dylos Count $P_{>2.5}$ (3)
A	57.6 (±21.9)	105.8 (±23.2)	2862.6 (±2524.4)	1647.2 (±1470.7)
B	123.2 (±34.1)	171.4 (±13.4)	4601.2 (±5236.7)	3042.2 (±3569.3)
C	116.8 (±31.4)	125.2 (±19.9)	3436.6 (±4326.0)	2440.8 (±3260.0)
D	58.4 (±19.6)	62.3 (±30.6)	183.6 (±127.7)	59.4 (±64.4)
E	47.8 (±17.7)	63.6 (±25.2)	280.6 (±161.6)	110.4 (±97.6)
F	125.8 (±15.8)	158.0 (±23.9)	5688.4 (±5212.5)	3685.4 (±3577.5)
G	40.3 (±13.4)	59.4 (±18.6)	187.0 (±140.6)	67.6 (±70.9)
H	58.2 (±23.5)	61.5 (± 30.9)	577.6 (±405.6)	259.0 (±219.0)

Appendix B-2. Correlation values for the first sampling collection.

Correlation (1a):(2)	Correlation (1a):(3)	Correlation (1b):(2)	Correlation (1b):(3)
0.908882	0.997093	0.97355	0.977508

Appendix C-1. Average of the SEM particle count and five-minute Dylos data for the second road sampling.

Site	High Stubs Average Count (1a)	Low Stubs Average Count (1b)	Dylos Count $P_{>0.5}$ (2)	Dylos Count $P_{>2.5}$ (3)
A.	38.25 (±7.1)	76.7 (±48.2)	5613.8 (±3581.2)	2632.3 (±2139.0)
B.	23.9 (±9.7)	27.5 (±8.8)	1136.6 (±150.8)	114.0 (±101.1)
C.	23.1 (±5.4)	33.6 (±7.9)	1709.8 (±567.9)	391.2 (±341.3)
D.	16.5 (±5.0)	17.1 (±5.4)	891.2 (±78.4)	26.2 (±5.6)
E.	34.4 (±10.1)	35.3 (±7.7)	2862.4 (±2872.7)	970.6 (±1960.2)
F.	26.8 (±7.3)	40.0 (±4.6)	2018.8 (±768.3)	688.0 (±498.8)
G.	81.0 (±27.0)	108.8 (±40.1)	5003.2 (±3912.1)	2768.0 (±2569.4)
H.	38.5 (±21.7)	37.3 (±15.0)	953.4 (±156.0)	82.4 (±80.0)

Appendix C-2. Correlation test for the second road sampling data.

Correlation (1a):(2)	Correlation (1a):(3)	Correlation (1b):(2)	Correlation (1b):(3)
0.687524	0.769401	0.8859	0.939066

Appendix D-1. Average of the SEM particle count and the five-minute Dylos data for the on campus sampling.

Site	High Stubs Average Count (1a)	Low Stubs Average Count (1b)	Dylos Count $P_{>0.5}$ (2)	Dylos Count $P_{>2.5}$ (3)
Busy				
F.	42.4 (±12.6)	54.5 (±23.1)	697.0 (±223.5)	246.2 (±95.6)
G.	51.8 (±18.3)	53.8 (±17.3)	697.0 (±196.5)	237.8 (±88.6)
H.	56.9 (±25.3)	73.2 (±23.8)	772.0 (±54.7)	119.4 (±42.3)
I.	90.0 (±54.0)	69.9 (±24.3)	706.8 (±109.9)	226.0 (±68.4)
Quiet				
F.	59.3 (±19.6)	41.4 (±28.8)	146.8 (±9.0)	10.6 (±3.0)
G.	52.8 (±20.7)	45.2 (±20.1)	311.2 (±21.1)	49.2 (±6.1)
H.	78.4 (±37.1)	61.3 (±30.3)	526.0 (±45.7)	77.2 (±29.3)
I.	86.3 (±17.2)	64.2 (±20.6)	712.8 (±47.4)	216.8 (±26.9)

Appendix D-2. Correlation test between the SEM sample count and the Dylos data.

Correlation (1a):(2)	Correlation (1a):(3)	Correlation (1b):(2)	Correlation (1b):(3)
0.187352321	0.109158459	0.826001569	0.468571135

Appendix E. SEM photos taken during viewing of the July Road Sampling.

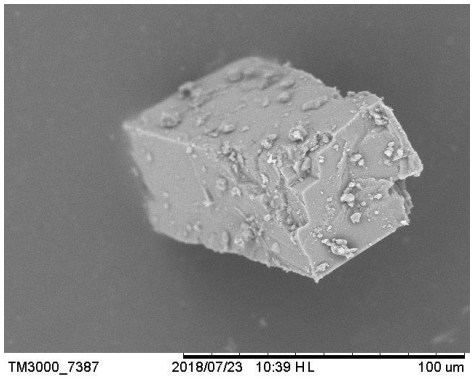

E-1. Mineral particle with smaller particles attached.

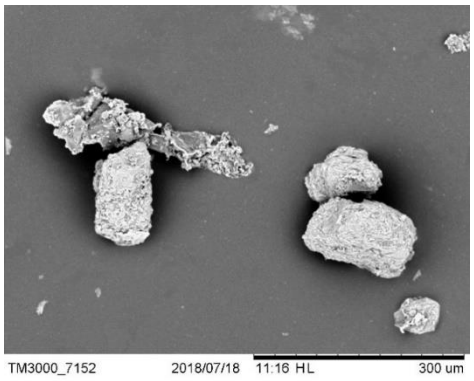

E-2. Inorganic particle cluster; most particles are around 100 µm.

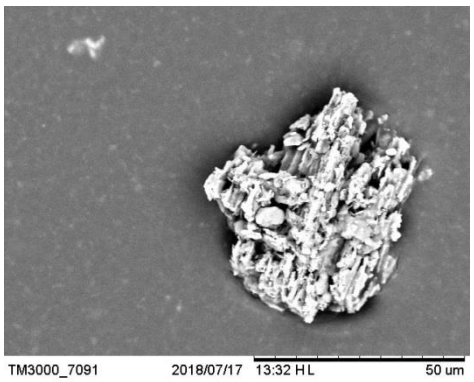

E-3. Particle aggregate with spiky appearance.

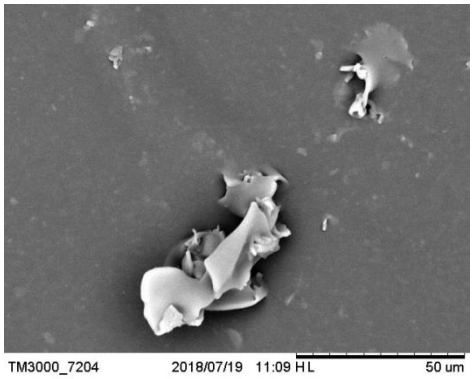

E-4. Film-like particles with folds.

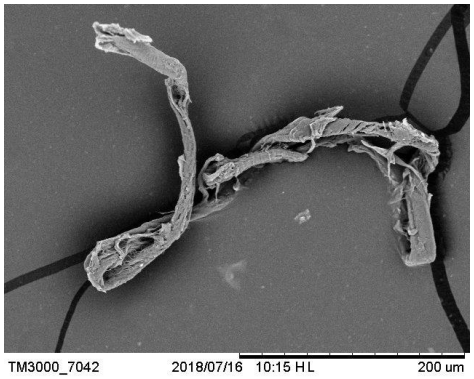

E-5. 400um particle with fiber-like appearance.

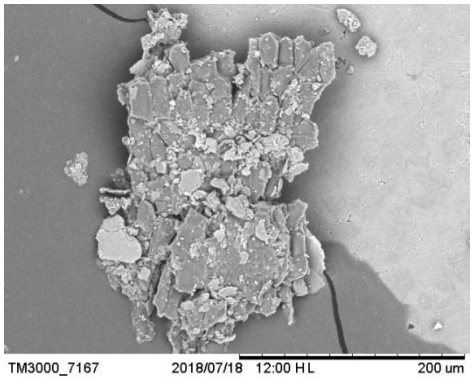

E-6. 240um particle with flaky appearance

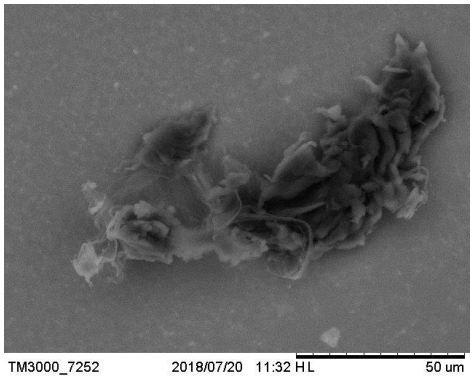

E-7. Fur-like particle that measured approximately 100 µm.

Appendix F. Particle photos from the August road sampling examination.

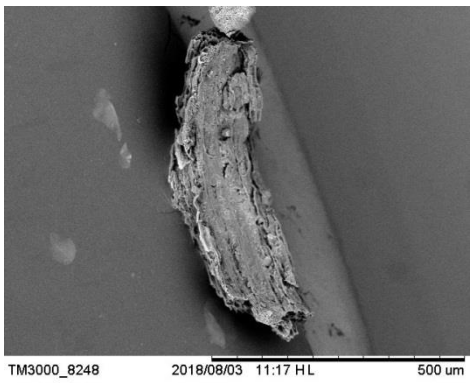

F-1. 550 µm, bark-like particle with wrinkled layers.

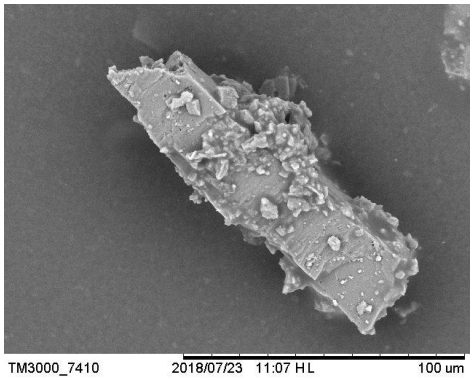

F-2. 100 µm mineral-like particle, with smaller particles adhered onto it.

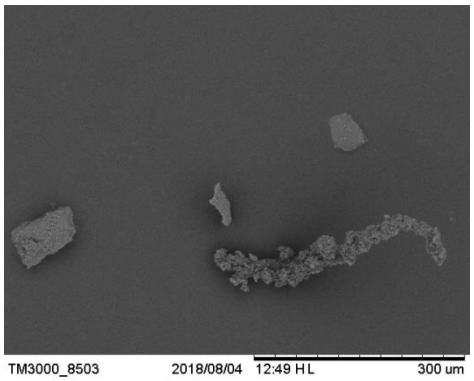

F-3. Particle cluster. One particle that was 300 µm was an aggregate of smaller particles.

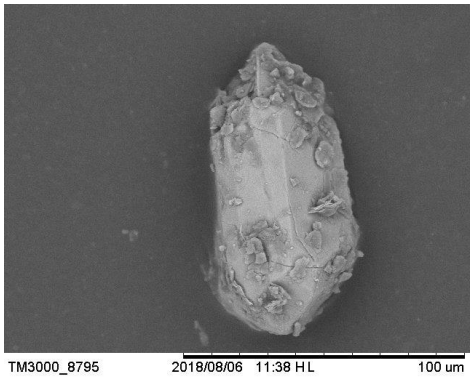

F-4. Mineral-like particle that was 90 µm, and also have small particles attached onto it.

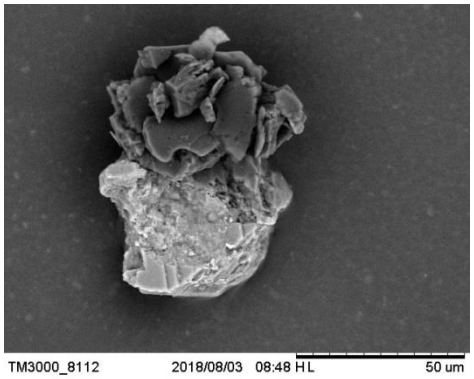

F-5. Two particles with different texture attached together.

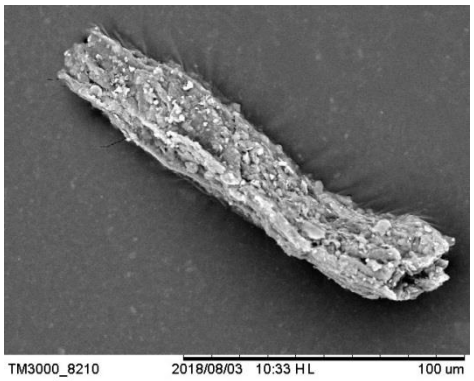

F-6. Bark-like particle with layers and numerous small particles attached onto it.

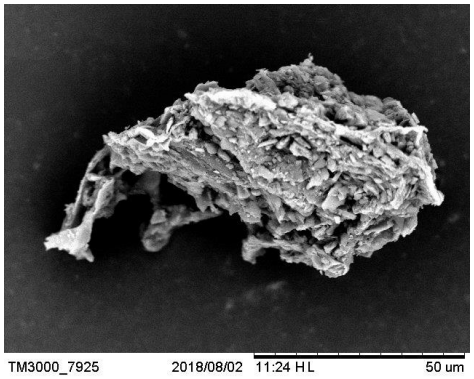

F-7. Particle with layer; formed by an aggregation of smaller particles.

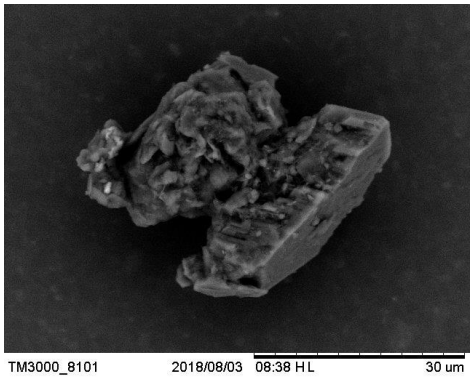

F-8. Two particles with mineral-like appearance.

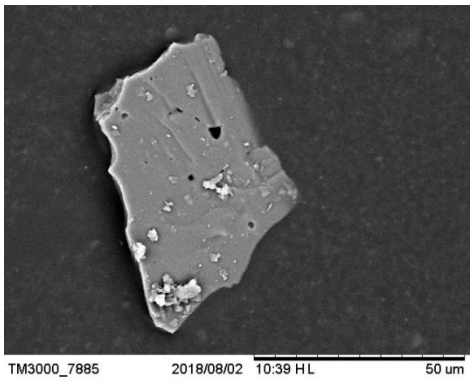

F-9. 50 µm, inorganic particle with small particles attached.

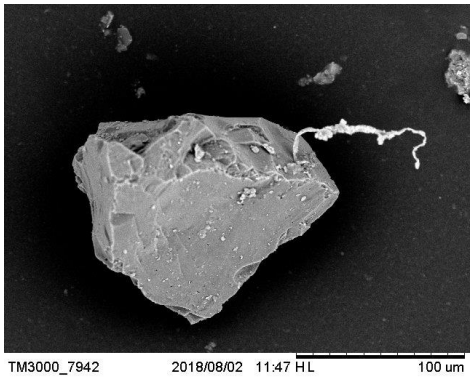

F-10. Inorganic particle with a fibrous particle attached with it.

F-11. Fibrous particle with tube-like subunits.

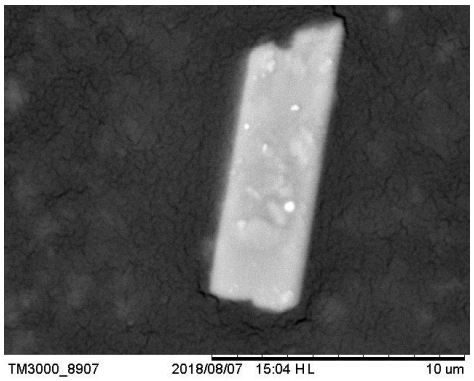

F-12. 10 µm particle with small particles attached onto it.

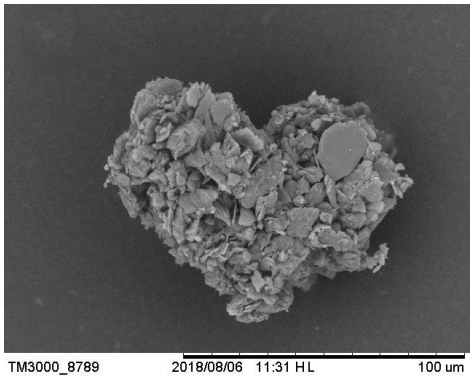

F-13. Particle aggregated from smaller, flaky particles.

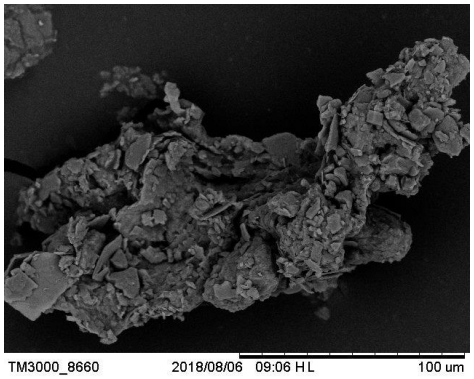

F-14. 200 µm particle with numerous smaller particles; most of the particles had flaky appearance.

Appendix G. SEM photos from the inbuilding sample examinations. Components of the indoor particles were slightly different compared to outdoor particulates. Most of them were also much smaller compared to the particulates found along the roads.

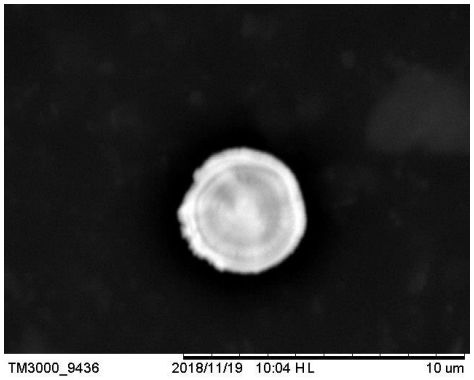

G-1. 5 µm particle with round and disc-like appearance.

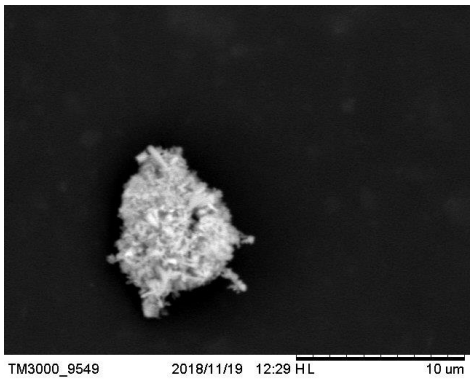

G-2. 10 µm particle with hair-like appearance.

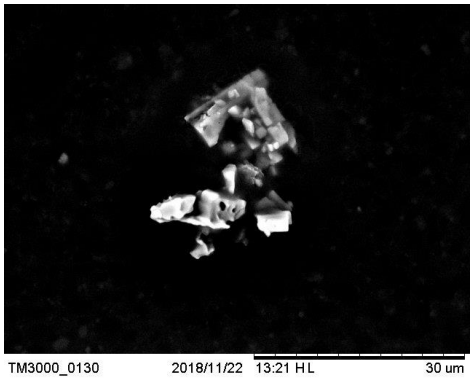

G-4. Particle cluster with crystalline and flaky appearances.

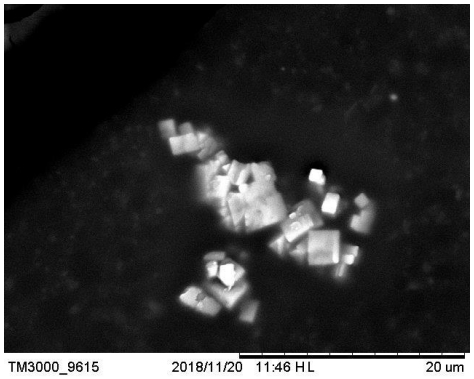

G-5. Particle cluster with similar crystalline appearances.

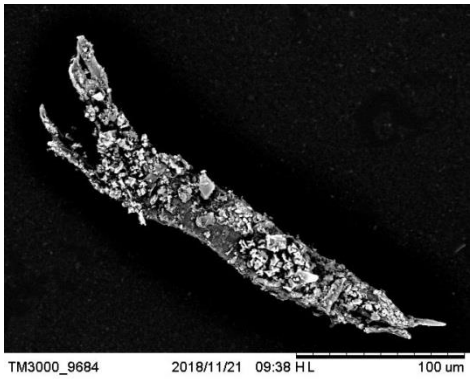

G-6. 300 µm particle with numerous small particles attached onto it.

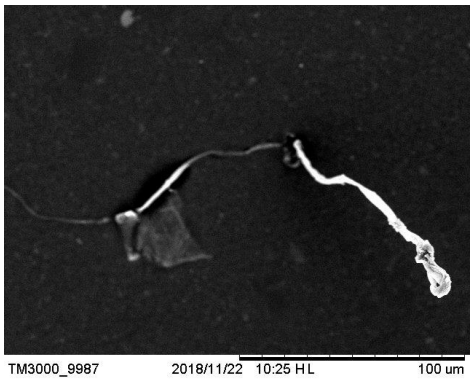

G-7. Long, filament particle that was about 200 µm in size.

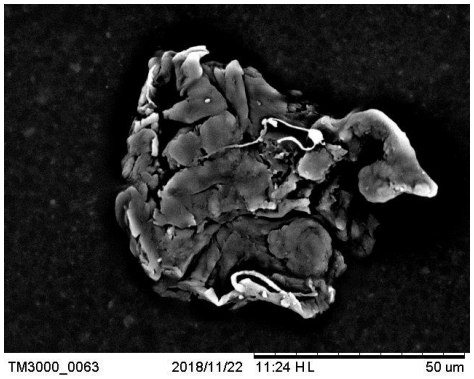

G-8. 50 µm particle with numerous folds and a filament attached onto it.

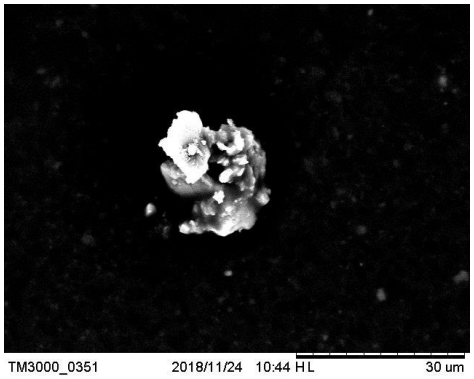

G-9. 28 µm particle aggregate.

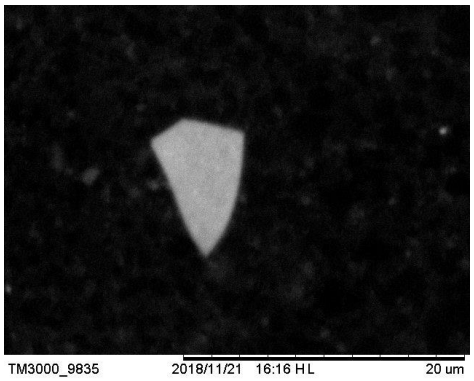

G-10. 10 µm, flat particle with sharp edges.

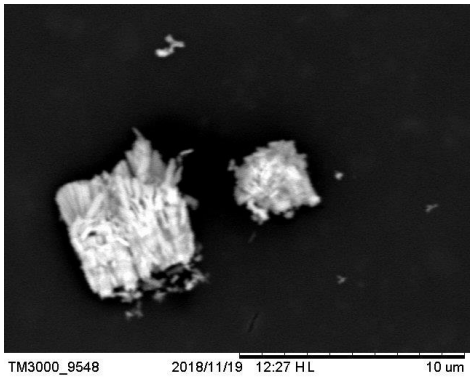

G-11. 5 µm particle with filamentous appearance. This particle was broken upon examination.